

A widely tunable parametric amplifier based on a SQUID array resonator

M. A. Castellanos-Beltran^a and K. W. Lehnert

*JILA, National Institute of Standards and Technology and the University of Colorado,
and Department of Physics, University of Colorado, Boulder, Colorado 80309*

(Dated: May 31, 2018)

Abstract

We create a Josephson parametric amplifier from a transmission line resonator whose inner conductor is made from a series SQUID array. By changing the magnetic flux through the SQUID loops, we are able to adjust the circuit's resonance frequency and, consequently, the center of the amplified band, between 4 and 7.8 GHz. We observe that the amplifier has gains as large as 28 dB and infer that it adds less than twice the input vacuum noise.

Josephson parametric amplifiers (JPAs) operate as ultralow noise microwave amplifiers. By detecting only one quadrature of a signal, degenerate parametric amplifiers can add even less noise than the minimum required by quantum mechanics when detecting both quadratures.¹ Josephson parametric amplifiers have been operated with near quantum-limited sensitivity² and have been used to squeeze both thermal and vacuum noise.^{3,4,5} In spite of these promising results, they have not been widely adopted since they suffer from two main disadvantages. They have both small dynamic range and narrow band gain; they are well suited to amplify signals only in a narrow range in both power and frequency, limiting their application. Furthermore, compelling applications that would benefit from a lower-noise microwave amplifier have only recently been developed. With the advent of quantum information processing using superconducting circuits,^{6,7} there is now a need for practical amplifiers that operate at the limits imposed by quantum mechanics.

The crucial element in a resonant-mode parametric amplifier is a circuit whose resonance frequency can be varied with time. If a reactive parameter oscillates at twice the resonance frequency, energy can be pumped into (or out of) the mode, realizing an amplifier. In practice, this time dependence is often generated through a nonlinear inductance or capacitance. If the nonlinear reactance is proportional to the intensity rather than the amplitude of the mode, then an intense pump tone applied at the resonance frequency ω automatically creates the necessary 2ω parametric oscillation. In analogy with optics, we describe this effect as a Kerr nonlinearity. The nonlinear current-dependent inductance of a Josephson junction,

$$L_j(I) = \frac{\hbar}{2eI_c} \frac{\arcsin(I/I_c)}{I/I_c} \quad (1)$$

provides such a Kerr nonlinearity, where I_c is the critical current of the junction, and I is the current flowing through it.

Because they are built from nonlinear resonant circuits, Josephson parametric amplifiers are inherently narrowband with limited dynamic range. Only signals close to the circuit's resonance frequency whose power is small compared to the pump can be linearly amplified. In this paper, we report a novel approach that addresses the limited bandwidth of Josephson parametric amplifiers. We create a JPA from a circuit whose resonance frequency can be adjusted between 4 and 7.8 GHz by applying a magnetic field. The amplifier is still narrowband, but the band center can be adjusted over an octave in frequency. With the amplifier, we demonstrate power gains as large as 28 dB. Furthermore, we can extract the

amplifier parameters by measuring the reflectance from the resonator and use them to accurately predict the amplifier's frequency-dependent gain. Finally, the sensitivity is improved by 16 dB when we place our parametric amplifier in front of a state-of-the-art microwave amplifier (HEMT). This improvement demonstrates that the parametric amplifier provides useful gain and operates much closer to the quantum limit than the HEMT amplifier.

The device we study consists of a quarter-wave coplanar-waveguide (CPW) resonator whose center conductor is an array of SQUIDs in series [Fig. 1(a)]. Two Josephson junctions in parallel form a SQUID, which behaves as a single junction with an effective $I_c = I_c^0 |\cos(\pi\Phi/\Phi_0)|$, where Φ/Φ_0 is the magnetic flux enclosed by the SQUID loop in units of flux quanta. By adjusting Φ through the SQUIDs, we can adjust the inductance per unit length of the coplanar waveguide (Eq. 1).⁸ We estimate I_c^0 for one SQUID to be $1.5 \mu\text{A}$. The resulting metamaterial has a zero-flux inductance per unit length of $L_l = 0.9 \text{ mH/m} \approx 700\mu_0$. The CPW has a capacitance per unit length of $C_l = 0.11 \text{ nF/m}$, yielding a phase velocity of $v_{ph} = 1/\sqrt{L_l C_l} = 0.01c$. We form a $\lambda/4$ resonator by shorting one end of the SQUID array CPW and capacitively coupling the other end to a 50Ω transmission line. The SQUID array behaves as a lumped element resonator^{9,10} close to its resonance frequency; it is not a distributed parametric amplifier.^{11,12}

The parametric amplifier is operated in reflection mode, as shown in Fig. 1(b). Two signal generators create two tones, a pump at frequency f_p and a signal at f_s . The two tones are summed before being injected into a dilution refrigerator operating at 15 mK. They are attenuated by 20 dB at 4 K. A directional coupler at 15 mK provides an additional 20 dB of attenuation and separates the incident tones from the reflected tones. Thus, including the 8-12 dB of loss from cables, incident tones and room-temperature Johnson noise are attenuated by about 50 dB.

Because of the nonlinearity of the metamaterial, the pump and signal tones mix. This mixing amplifies the signal and creates an idler, or intermodulation tone, at a frequency $f_I = 2f_p - f_s$. To further amplify the signals coming out of our resonator, we use a cryogenic HEMT amplifier with noise temperature $T_N = 5 \text{ K}$ and another set of low noise amplifiers at room temperature. An isolator at base temperature prevents the noise emitted by the input of the HEMT amplifier from exciting the JPA. Amplitudes and phases of the signals at the output of the room temperature amplifiers are recovered with an IQ demodulator whose local oscillator (LO) can be provided by either microwave generator.

Before operating the parametric amplifier, we characterize the resonator's reflectance with just a pump tone. We first study the flux dependence of the resonator by measuring the real (I) and imaginary (Q) part of the reflection coefficient Γ as a function of frequency. The resonance frequency f_{res} is identified by a dip in $|\Gamma|$. Figure 2(a) shows how the resonance frequency behaves as a function of Φ/Φ_0 . The applied flux increases L_l , reducing v_{ph} and consequently f_{res} .

By measuring Γ as a function of frequency and incident power, we obtain the linear and nonlinear resonator parameters [Fig. 2(b)]. At low enough incident power P , where the resonator response is linear, we extract the damping rates associated with the coupling capacitor γ_1 and the linear dissipation in the resonator γ_2 . We extract these from the halfwidth $[(\gamma_1 + \gamma_2)/2\pi]$ and the depth of the dip $[(\gamma_2 - \gamma_1)/(\gamma_2 + \gamma_1)]$ in $|\Gamma|$ at the resonance frequency $\omega_0 = 2\pi f_{res}$. For a flux of $\Phi = 0.2\Phi_0$, we find the resonator's linear parameters $f_{res} = 6.952$ GHz, $\gamma_1/2\pi = 1.9$ MHz, and $\gamma_2/2\pi = 1.1$ MHz. As we increase the pump power, the Kerr nonlinearity makes the resonance frequency decrease according to the equation $\omega_0 - \omega_m + KE = 0$, where ω_m is the frequency at which Γ is minimum, K is the Kerr constant, and E is the energy stored in the resonator.¹³ Above the critical power P_c , Γ is discontinuous, and the resonators response is bistable. From the frequency and power dependence of Γ , we estimate the critical power and Kerr constant to be $P_c = 3 \pm 1.3$ fW and $\hbar K = -1.6 \pm 0.7 \times 10^{-5}$, respectively. The large uncertainty comes from the 4 dB uncertainty of the incident power on the resonator. From Appendix A in Ref. 13, we can calculate the Kerr constant from the number of SQUIDs and their I_c . The expected value for the Kerr constant is $\hbar K = -1 \times 10^{-5}$, in agreement with our measurement. To model more completely the behavior of the resonator, we also include a nonlinear dissipation term $\gamma_3 = 0.027|K|$, which is the imaginary part of the Kerr constant. From the physical characteristics of the resonator, we can predict f_{res} , γ_1 , and K ; however we do not yet understand the physical origin of γ_2 and γ_3 .

The analysis of the parametric amplifier follows closely the theory developed by Yurke and Buks for parametric amplification in superconducting resonators.¹³ In their model, the Kerr nonlinearity is provided by the intrinsic kinetic inductance of a superconducting film,¹⁴ while in our case it arises from the nonlinear Josephson inductance of the SQUIDs (Eq. 1).

The intermodulation gain (IG) and direct gain (DG) can be predicted from the resonator's parameters. We define DG as the ratio between the reflected signal power with the pump

on and the incident signal power; IG is the ratio between the intermodulation tone and the incident signal. To verify the behavior of the parametric amplifier, we operate it in the nondegenerate mode and measure the frequency dependence of both gains in two different ways. In the nondegenerate mode, the signal and the pump frequencies are different, and the generator that creates the signal tone also provides the LO to the demodulator. In the first test, we apply the pump at a frequency close to ω_m and analyze DG and IG as we detune the signal frequency from the pump by an amount δf . In Figs. 3(a) and 3(b), we plot both IG and DG as a function δf for two different pump powers. We also plot the predictions from the theory in Ref.¹³ where the parameters in the theory are extracted from the measurements of Γ . From this plot, we estimate the 3 dB bandwidth to be about 300 kHz when DG and IG are 18 dB. Next, we measure IG and DG as a function of pump detuning, *i.e.*, the difference in frequency between the applied pump and f_{res} . In this test, the signal and the pump frequency differ by a fixed amount, $\delta f = 10$ kHz, [Figs. 3(c) and 3(d)]. From the agreement seen in Fig. 3, we conclude that Ref. 13 provides an appropriate model for our device.

For $f_{res} = 6.95$ GHz ($\Phi = 0.2\Phi_0$), we have also operated the JPA in a doubly degenerate mode where the pump and the signal frequencies are the same. In this mode, the gain of the parametric amplifier is sensitive to the phase between the pump and the signal. To measure this phase dependence, we amplitude modulate the signal at 20 kHz and adjust the phase of the pump relative to the signal. We define the gain as the ratio of the AM modulation sideband power with the pump on and pump off. Because the local oscillator frequency and the pump frequency are the same, the signal and intermodulation tones are added at the output of the demodulator, giving a total gain 3 dB larger than either DG or IG. In degenerate mode, the gain can be 3 dB larger than in nondegenerate mode if the phase between the pump and signal is tuned for maximum gain. The phase dependence of the gain for a pump power close to P_c is shown in Fig. 4(a); there it is evident that we see deamplification, a hallmark of degenerate parametric amplifiers. In Fig. 4(b), we plot the power spectral density (PSD) of the demodulated signal with the pump off and pump on for $P = 0.95P_c$, where the signal-pump phase has been adjusted for maximum gain (28 ± 0.2 dB). At this gain, the HEMT amplifier's input noise is overwhelmed by the noise at the output of the parametric amplifier, effectively improving the signal-to-noise ratio (S/N) by 16 ± 0.4 dB. A definitive measurement of the noise added by our parametric amplifier will

require a calibrated noise source. We have not yet completed this measurement. However, by measuring the S/N with the pump off, we find that the noise referred to the input of the HEMT is $T_N = 12 \pm 5$ K. From the S/N improvement with the pump on, we estimate the total noise referred to the input of the JPA as 300 ± 130 mK. This value suggests that the parametric amplifier adds an amount of noise comparable to the vacuum noise ($\hbar f_{res}/2k_B = 166$ mK), which must be present at the input of the JPA.

To demonstrate the tunability of the JPA, we also test the performance of the amplifier at lower frequencies. For example, for $\Phi = 0.35\Phi_0$, the resonance frequency is $\omega_0/2\pi = 5.203$ GHz. A similar analysis as the one described for $\Phi = 0.2\Phi_0$ gives the following parameters: $\gamma_1/2\pi = 0.95$ MHz, $\gamma_2/2\pi = 0.85$ MHz, $P_c = 0.5 \pm 0.2$ fW, $\hbar K = -9 \pm 4 \times 10^{-5}$ and $\gamma_3 = 0.145 |K|$. The increase in the nonlinear loss degrades the performance of the amplifier, making the measured gains smaller than the ones at 6.95 GHz. The highest IG and DG observed at this frequency are both 12 dB.

Although the power-handling capacity of this device is low (critical powers of the order of a few femtowatts), its performance is appropriate for amplifying the signals generated by superconducting qubits. By virtue of the tunability of our amplifier's band, it can be brought into resonance with a second high-Q superconducting resonator used to study superconducting qubits as in Refs. 6 and 7. For more general applications where larger signals need to be amplified, similar parametric amplifiers could be used if the critical current of the SQUIDs is made larger.

In conclusion, we have demonstrated a widely tunable parametric amplifier based on a coplanar waveguide resonator whose inner conductor is made from a SQUID array. We have observed tunability over an octave and gains as high as 28 dB. Although the resonator is composed of discrete elements, its behaviour is well described by a continuum theory of parametric amplification.¹³ Finally we have demonstrated that the JPA is 16 dB more sensitive to a weak microwave signal than a low-noise HEMT amplifier, suggesting that the JPA adds less than twice the vacuum noise.

The authors thank S. M. Girvin for valuable conversations. K. W. Lehnert is a member of NIST's Quantum Physics Division.

^a Electronic mail: castellm@colorado.edu

- ¹ H. Takahasi, *Adv. Comm. Syst.* **1**, 227 (1965).
- ² B. Yurke, L. R. Corruccini, P. G. Kaminsky, L. W. Rupp, A. D. Smith, A. H. Silver, R. W. Simon, and E. A. Whittaker, *Phys. Rev. A* **39**, 2519 (1989).
- ³ B. Yurke, *J. Opt. Soc. Am. B* **4**, 1551 (1987).
- ⁴ B. Yurke, P. G. Kaminsky, R. E. Miller, E. A. Whittaker, A. D. Smith, A. H. Silver, and R. W. Simon, *Phys. Rev. Lett.* **60**, 764 (1988).
- ⁵ R. Movshovich, B. Yurke, P. G. Kaminsky, A. D. Smith, A. H. Silver, R. W. Simon, and M. V. Schneider, *Phys. Rev. Lett.* **65**, 1419 (1990).
- ⁶ A. Wallraff, D. I. Schuster, A. B. L. Frunzio, R.-S. Huang, J. Majer, S. Kumar, S. M. Girvin, and R. J. Schoelkopf, *Nature* **431**, 162 (2004).
- ⁷ D. I. Schuster, A. A. Houck, J. A. Schreier, A. Wallraff, J. M. Gambetta, A. Blais, L. Frunzio, J. Majer, B. Johnson, M. H. Devoret, S. M. Girvin, and R. J. Schoelkopf, *Nature* **445**, 515 (2007).
- ⁸ D. B. Haviland and P. Delsing, *Phys. Rev. B* **54**, 6857 (1996).
- ⁹ S. Wahlsten, S. Rudner, and T. Claeson, *J. Appl. Phys.* **49**, 4248 (1977).
- ¹⁰ M. J. Feldman, P. T. Parrish, and R. Y. Chiao, *J. Appl. Phys.* **46**, 4031 (1975).
- ¹¹ M. Sweeny and R. Mahler, *IEEE Trans. Magn.* **21**, 654 (1985).
- ¹² B. Yurke, M. L. Roukes, R. Movshovich, and A. N. Pargellis, *Appl. Phys. Lett.* **69**, 3078 (1996).
- ¹³ B. Yurke and E. Buks, *J. Lightwave Technol.* **24**, 5054 (2006).
- ¹⁴ E. A. Tholen, A. Ergul, E. M. Doherty, F. M. Weber, F. Gregis, and D. B. Haviland, *cond-mat/0702280* (2007).

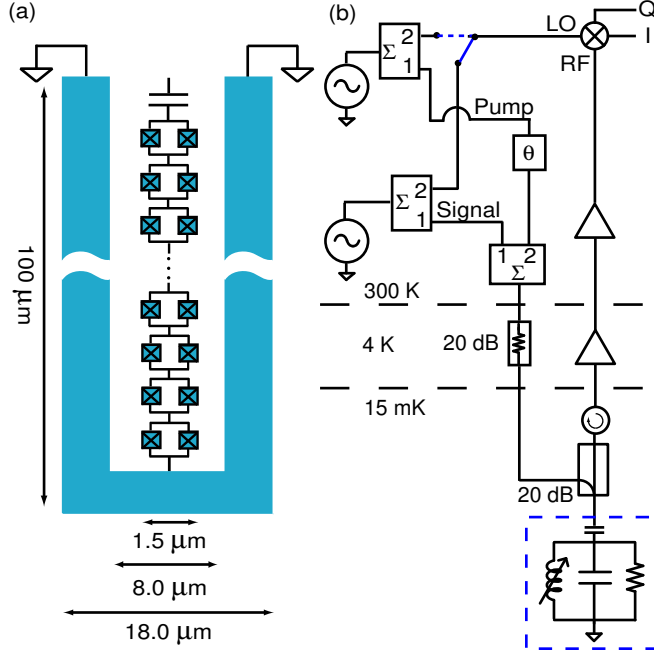


FIG. 1: Device diagram and measurement schematic. (a) The device's center conductor is a series array of 400 SQUIDs. The resonator's ground plane is made out of aluminum, and the SQUIDs are made from Al/AlOx/Al junctions. They are fabricated using E-beam lithography and double angle evaporation on an oxidized silicon substrate. (b) Simplified measurement schematic. We model the resonator as an RLC circuit, as shown in the dashed box.

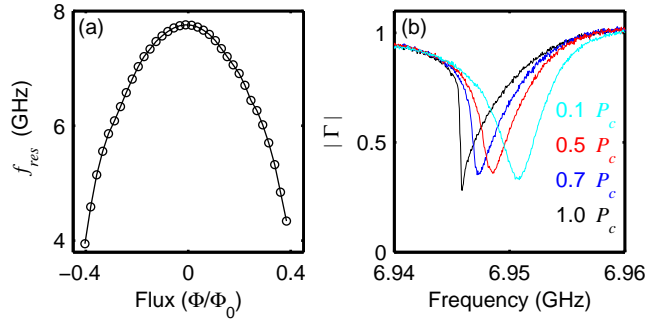


FIG. 2: Flux and power dependance of the resonance circuit. (a) Resonance frequency as a function of flux. (b) Reflection coefficient magnitude as a function of frequency at different pump powers for $\Phi = 0.2\Phi_0$.

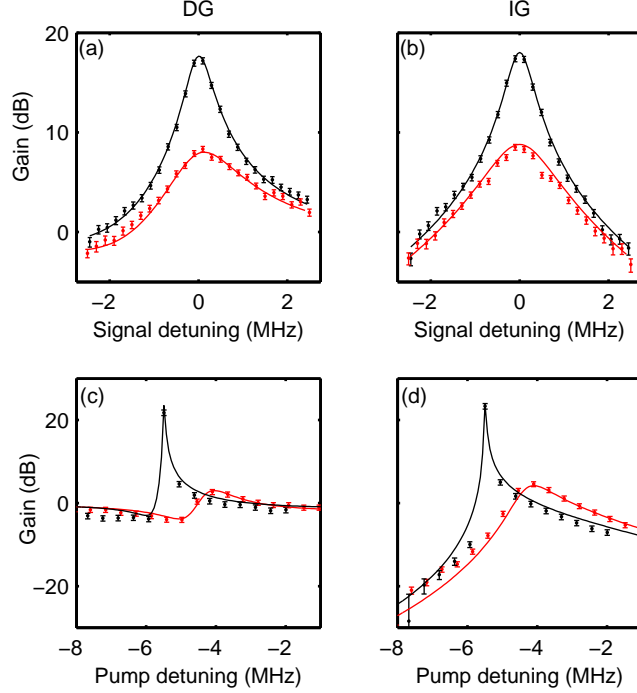


FIG. 3: Performance of the amplifier in nondegenerate mode. (a) and (b) DG and IG as functions of signal detuning (points) and predictions of Ref. 13 (lines) for two different pump powers. DG and IG for $P = 0.9 P_c$ (black) and for $P = 0.75 P_c$ (red). (c) and (d) DG and IG as functions of pump detuning (points) for $P = 0.95 P_c$ (blue) and $P = 0.5 P_c$ (red) and prediction (lines) of Ref. 13.

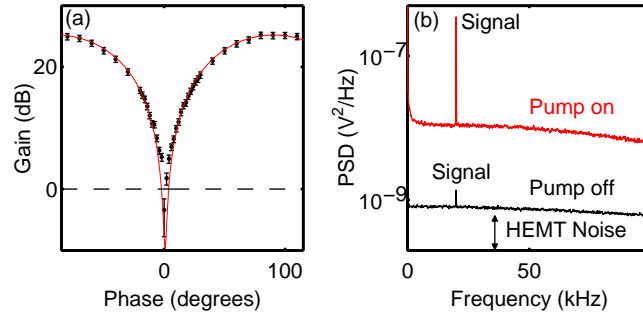


FIG. 4: Performance of the amplifier in degenerate mode. (a) Gain as a function of the phase between the pump and the signal (points) and prediction (line) from Ref. 13 ($P = 0.9 P_c$). (b) Power spectral density of the demodulator output for the cases when the pump is on ($P = 0.95 P_c$) and off. The gain in this case is 630 ± 30 (28 ± 0.2 dB). The applied signal power is $1.6 \pm 0.7 \times 10^{-20}$ watts.